Proceedings of the 2018 Design of Medical Devices Conference
DMD2018
April 9-12, 2018, Minneapolis, MN, USA

DMD2018-6911

REALIZATION OF A STATICALLY BALANCED COMPLIANT PLANAR REMOTE CENTER OF MOTION MECHANISM FOR ROBOTIC SURGERY

Karthik Chandrasekaran, Adarsh Somayaji, and Asokan Thondiyath
Department of Engineering Design,
Indian Institute of Technology Madras,
Chennai 600036, India

BACKGROUND

Robot assisted minimally invasive surgery helps overcome some of the limitations like limited dexterity, fulcrum effect, and lack of 3D vision in manual laparoscopic procedures [1]. A Remote Centre of Motion (RCM) mechanism is an essential part of tele-operated surgical robots. An RCM mechanism enables a rigid surgical tool to maintain a kinematic constraint about the insertion point on a patient's body [2]. It permits a surgical tool to pivot only about the insertion point and prevents tool translation about the insertion point [3]. A parallelogram architecture based RCM mechanism is one of the most commonly used RCM mechanisms in surgical robots [4] due to its simplicity and large usable range of motion. Commercially available surgical robots such as da Vinci™ from Intuitive Surgical Inc. [5] use synchronous transmission [2] based passive RCM mechanism as a substitute for parallelogram based RCM.

Currently available RCM mechanisms for surgical robots use rigid body linkages with traditional mechanical joints that are susceptible to joint wear, lubrication issues, backlash, and loss of haptic feedback due to joint friction. To overcome some of the issues associated with rigid links, compliant mechanisms are proposed as an ideal substitute for traditional joints in surgical instruments, as pointed out by Kota et al. [6]. Existing flexure-based planar RCM mechanisms that can be found in literature have limited range of motion [7] [8]. However, surgical robots require an RCM mechanism with large range of motion. Therefore, a large deflection compliant RCM mechanism could be a potential replacement for a conventional rigid body based RCM mechanism. Also, if the RCM mechanism could be made monolithic, it would have the added advantage of reduced weight which is crucial for any surgical robot. Additionally, a compliant RCM could enable sensor less force estimation of the surgical tool using motor current [9]. This paper focuses on realizing a one Degree of Freedom (DOF) statically balanced, monolithic compliant planar RCM mechanism that can be used in tele-operated surgical robots, and automated endoscope holders.

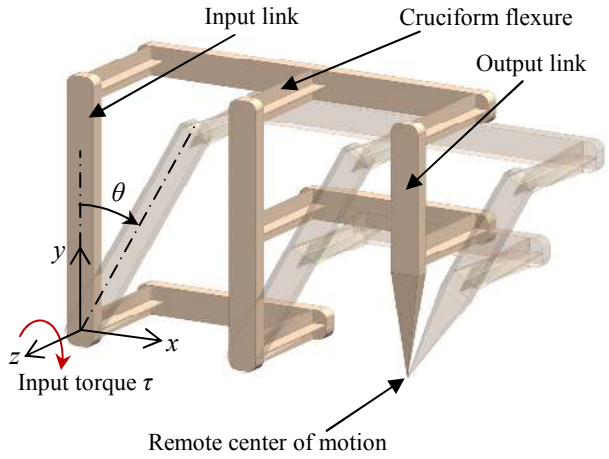

Figure 1. Conceptual model of cruciform flexure based remote center of motion mechanism

METHODS

A Computer Aided Design (CAD) of the proposed flexure based monolithic design of RCM mechanism is shown in figure 1. The RCM mechanism in its deflected position is also shown in figure 1 and it can be seen that the remote center of motion remains fixed in space. Since the mechanism should undergo large deflection, flexures capable of large deflection only can be used for the design. Corner filleted flexure, cruciform flexure,

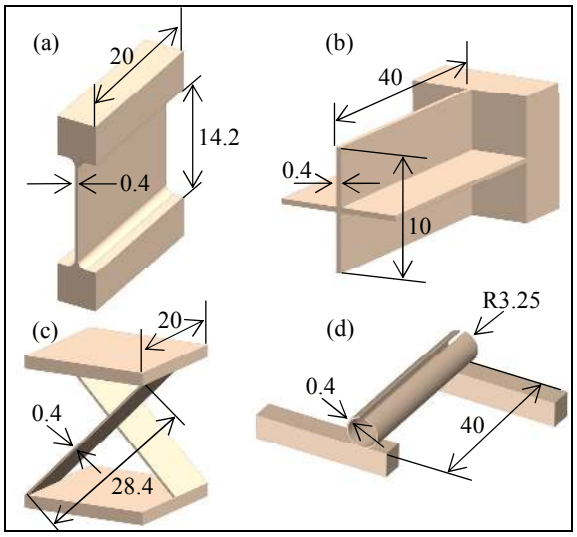

Figure 2. Dimensions (in mm) of chosen large deflection flexures (a) Corner filleted flexure (b) Cruciform flexure (c) Cross pivot flexure (d) Split tube flexure

cross pivot flexure and split tube flexure [10] were considered here for the design of the RCM mechanism. The desired range of motion (θ) of the RCM mechanism is considered to be ±40 degree [11] from vertical. The proposed compliant RCM mechanism was realized through Rigid Body Replacement (RBR) [12] by replacing all the conventional hinges of a parallelogram based RCM by large deflection compliant flexures. To identify the most suitable flexure for the mechanism, a comparison was made between the flexures with the parasitic drift of each flexure as the prime selection criteria. Parasitic drift of any chosen flexure would cause drift of the remote center of motion which is detrimental to the RCM performance.

Table 1 Comparison of different large deflection flexures

Flexure	Drift of RCM along x axis (mm)	Drift of RCM along y axis (mm)
Corner filleted	2.94	-1.77
Cruciform	0.89	-2.12
Cross pivot	5.44	-2.68
Split tube	0.73	-4.94

To study the drift of the RCM point that would be caused by each flexure, parallelogram RCM mechanisms, based on all the four type of flexures were modelled using RBR method. Figure 2 shows the flexures considered for analysis along with their dimensions. Revolute stiffness of each flexure was maintained to be the same for fair comparison. The thickness was kept the same for every flexure and the longest dimension of every flexure was limited to 40mm and the other dimensions were varied to keep the revolute stiffness of all the flexures the same. The material used for the flexure was Polylactic acid (PLA) [13]. The size of the RCM mechanism was restricted to fit within a rectangle of size 130x90 mm. Separate Finite Element Analysis (FEA) using Abaqus™ software was carried out on all the four models. Table 1 lists the drift of the remote center of motion in the x-y plane of each flexure for an angle of deflection (θ) of 40 degree in the clockwise direction. The out of plane drift of the RCM point was not considered as the links of the RCM mechanisms in parallel planes remained reasonably parallel in all the simulations. It was found that the mechanism with the cruciform flexure causes the RCM mechanism to have the least net drift of the remote center of motion. Also, it has superior off axis stiffness compared to other flexures and hence this flexure was chosen for the RCM mechanism. The stresses in the cruciform flexure were found to be well within the elastic limit of the material for the considered deflection.

Static balancing

Since flexures achieve mobility by deformation, they store strain energy when displaced from their neutral position and hence are not energy free [14] [15]. In the proposed RCM mechanism, there are seven cruciform flexures which store energy when deflected and need constant holding torque from an external actuator to maintain a given position. This is not acceptable from a safety standpoint since the mechanism would move if the actuator torque is removed. Energy exchange from an auxiliary body can be utilized to make the flexure to have zero stiffness and thus statically balanced [14]. Additionally, static balancing would reduce actuation force input, thus reducing actuator size. Since there are seven cruciform flexures placed in the parallelogram configuration, all flexures undergo same angular deflection when an input torque is applied at the input link. It is necessary to find a method for balancing the RCM mechanism and the method adopted is explained below.

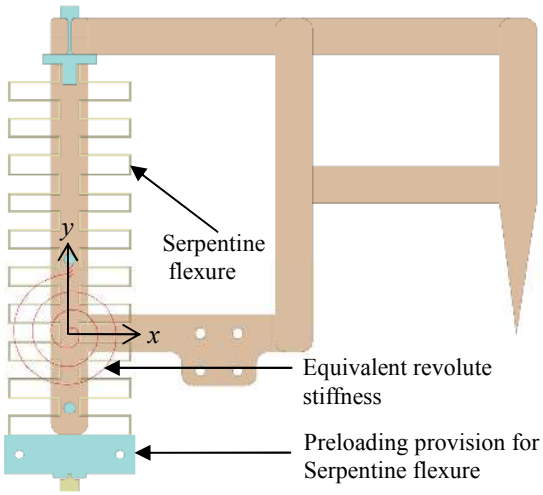

Figure 3. Static Balancing of RCM mechanism with a serpentine flexure

Since all the joints of the RCM undergo same angular deformation, an equivalent stiffness of the entire mechanism about the rotational axis of input link can be found by adding the stiffness of each individual flexure of the RCM mechanism. This equivalent stiffness is taken at the axis of rotation of the input link as shown in figure 3. The equivalent stiffness of the mechanism is seven times the revolute stiffness of a cruciform flexure and the expression can be found in Smith [16]. Therefore the static balancing of the proposed mechanism can be simplified to a spring to spring balancing problem. A negative stiffness mechanism is needed to counter balance the positive stiffness offered by the RCM mechanism [17]. Adding an auxiliary preloaded torsional spring to the input link of the RCM mechanism cannot counter-balance the mechanism as it would simply act as another spring added in parallel to the RCM mechanism. A toggling mechanism is required to realize a negative stiffness mechanism. Static balancing designs for compliant mechanisms proposed by Aguirre et al. [17] and Bruyas et al. [18] utilize a toggling mechanism with a linear spring to realize a negative stiffness mechanism. Since our design aims to create a monolithic mechanism, we have utilized a serpentine flexure as a linear spring as shown in figure 3. The linear stiffness of the serpentine flexure along *y*-axis can be calculated using relations found in Fedder [19].

A separate FEA simulation was carried out for the serpentine flexure to ensure that the stresses caused by preloading the flexure would be well within the allowable limit of the material [13] of the flexure. From figure 3, the length, stiffness, and preload of the counterbalancing serpentine flexure were calculated using a numerical optimization procedure [18] which aims to minimize the net moment of the whole system about the input link's rotational axis (*z*-axis).

Prototype

Figure 4 shows the RCM mechanism without the serpentine flexure. The prototype of the proposed mechanism was 3D printed using fused filament fabrication technique on a standard 3D printer. The serpentine flexure was printed separately with

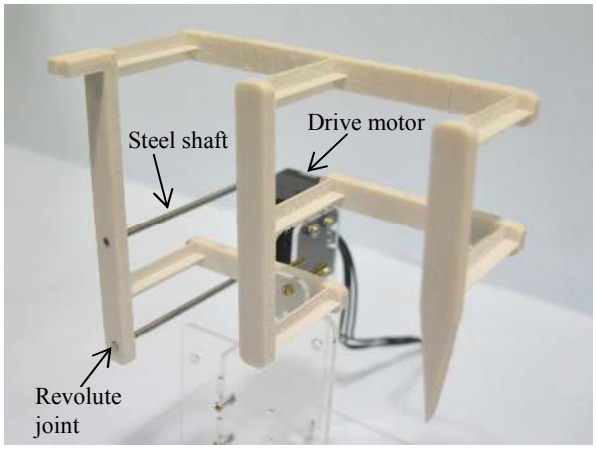

Figure 4. 3D printed RCM mechanism with drive motor

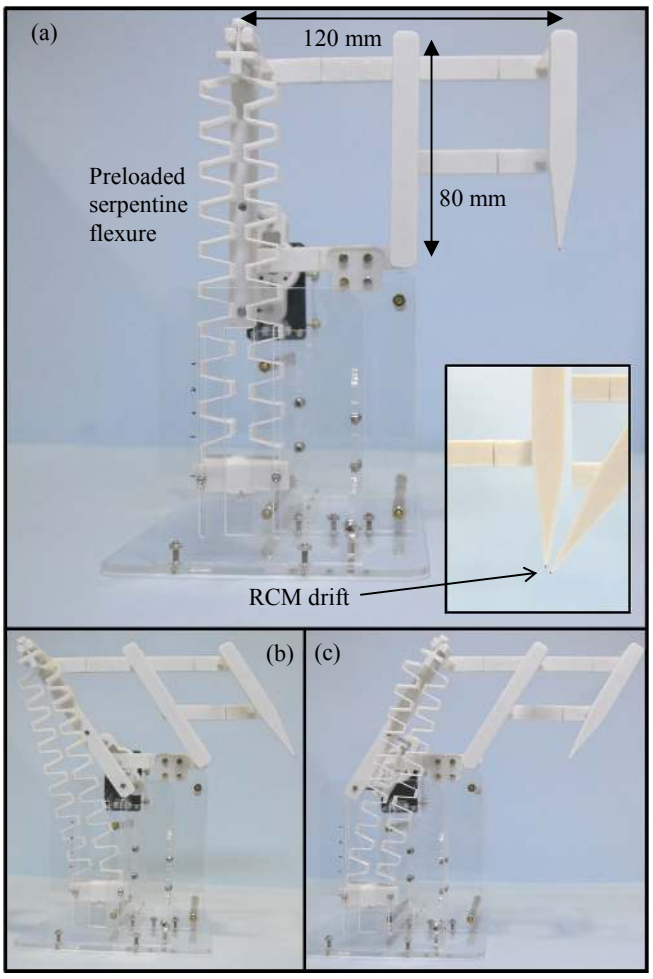

Figure 5. Statically balanced prototype demonstrating its range of motion

corner filleted flexures at both its ends and connected to the RCM mechanism by a dovetail joint to ensure a positive lock. The mechanism is driven by a Dynamixel™ X430 servo motor, which has position and torque control capability. The drive motor is directly coupled to the input link by a pair of steel shafts. The shafts are connected to the input link by revolute joints. This direct drive configuration was chosen, since using a belt drive or similar drive method would put additional radial load on the assembly and influence the drift of the flexure. Figure 5 shows the statically balanced RCM mechanism with the preloaded serpentine flexure. The mechanism was mounted on a laser cut acrylic structure for testing. Inset figure in figure 5 (a) shows two superimposed images of RCM mechanism taken in the neutral position and fully deflected position.

RESULTS

Static balance test

The serpentine flexure was preloaded by stretching and locking its free end as shown in Figure 5. This stored strain

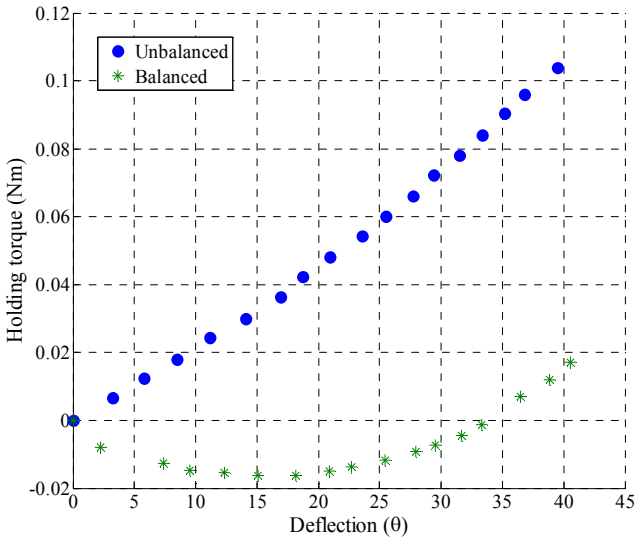

Figure 6. Comparison between statically balanced and unbalanced RCM mechanism

energy serves to provide static balancing for the RCM mechanism. Several tests were carried out using a separate test setup and a calibrated vision system to track the deflection of the input link of the RCM mechanism. The RCM mechanism was tested with and without the serpentine flexure with 5 trials each. The mechanism was moved in a quasi-static manner and the torque required to hold the mechanism at a particular angular deflection was recorded with a separate force gauge. The mean of the readings of all the trials is shown in figure 6. The maximum standard deviation for the unbalanced and balanced trials was found to be 0.0019 and 0.0014 respectively. It can be seen from figure 6 that the peak torque at maximum deflection has come down by 83 percent for the balanced RCM mechanism.

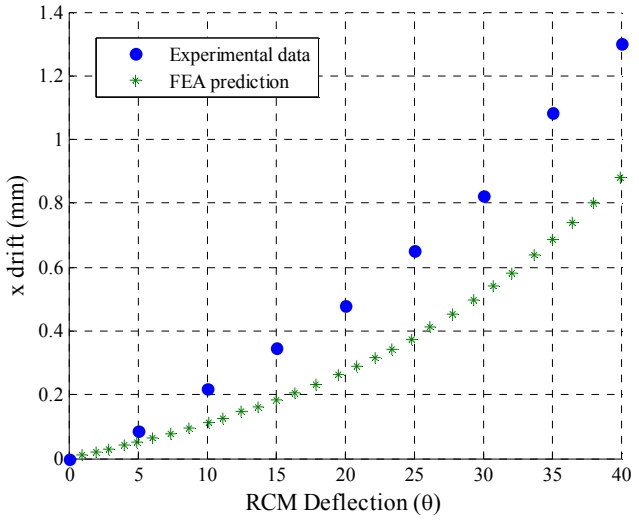

Figure 7. Drift along *x*-axis of the RCM point of the RCM mechanism

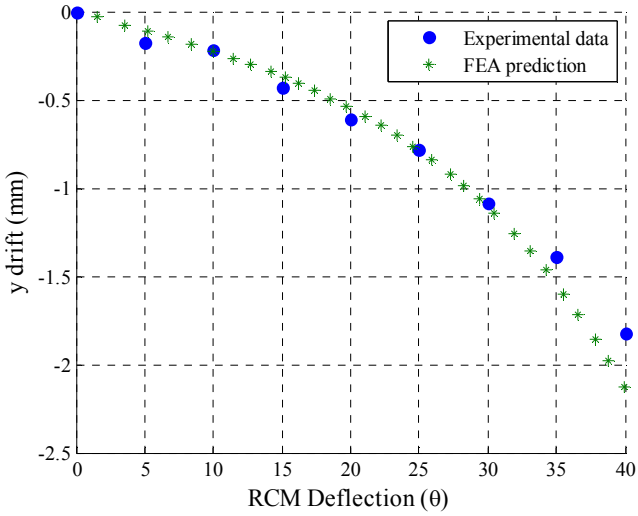

Figure 8. Drift along *y*-axis of the RCM point of the RCM mechanism

RCM drift test

The drift of the remote center of motion of the RCM mechanism was tracked using a calibrated vision system. The input link of the RCM mechanism was given angular displacement in finite intervals in clockwise direction and the drift of the RCM point was recorded. Figures 7 and 8 show the planar drift of the RCM point for half the range of motion of the mechanism. A total of 5 trials were conducted and the mean value is reported in the figures. The maximum standard deviation for drift along *x* and *y* axes were 0.15. Separate FEA simulations were carried out to assess drift of the RCM. Figures 7 and 8 show both the experimental and FEA prediction. It can be seen that there is good correspondence for drift in *y*-axis. The difference between the drift of the RCM point between the FEA simulation and the experimental result along the *x*-axis could be due to the assumption made in the FEA simulation that the material is linear and isotropic. A nonlinear model for the polymer material could better capture the behavior of the polymer used for 3D printing. The mechanism also exhibited asymmetry of the RCM point drift when rotated to the other half of the workspace.

INTERPRETATION

A compliant RCM mechanism was realized through RBR with large deflection cruciform flexure. Preliminary testing with prototype showed that the RCM is capable of large deflections required for robotic surgery. Additional FEA simulations confirmed that scaling the mechanism does not significantly change the RCM drift. Experimental evaluation of the mechanism reveals that the drift of the RCM of the proposed mechanism was minimal. Static balancing was also performed to make the mechanism energy free and hence improve safety and reduce torque input for actuation. An additional flexure for enabling rotation about the *x*-axis can be provided for out of

plane motion of the tool connected to the RCM mechanism. Further design changes are in the works for possibly achieving static balancing of the mechanism without any auxiliary body by utilizing preloaded flexures. Efforts are also underway to study the effect of hysteresis on drift of the RCM point and torque input to the mechanism when reversing the direction of motion of the RCM mechanism.

REFERENCES

[1] Lanfranco, A. R., Castellanos, A. E., Desai, J. P., Meyers, W. C., 2004, "Robotic Surgery", Annals of Surgery, Vol. 239, Issue 1, pp. 14-21.

[2] Zong, G., Pei, X., Yu, J., Bi, S., 2007, "Classification and type synthesis of 1-DOF remote center of motion mechanisms," Mechanism and Machine Theory, Vol. 43, Issue 12, pp.1585-1595.

[3] Taylor, R. H., Stoianovici, D., 2003, "Medical robotics in computer-integrated surgery," IEEE Transactions on Robotics, Vol. 19, Issue 5, pp. 765-781.

[4] Taylor, R. H., Funda, J., David, D., Grossman, Karidis, J., P, LaRose, D., A, 1995, "Remote center-of-motion robot for surgery," U.S. Patent No.5397323 A.

[5] Intuitive Surgical, Inc., 2017, "da Vinci robot," accessed on October 28, 2017, https://www.intuitivesurgical.com/products/davinci_surgical_system/.

[6] Kota, S., Lu, K.-J., Kreiner, Z., Trease, B., Arenas, J., and Geiger, J., 2005, "Design and Application of Compliant Mechanisms for Surgical Tools," ASME J. Biomech. Eng., Vol. 127, Issue 6, pp. 981–989. doi:10.1115/1.2056561.

[7] Lipkin, H., Ciblak, N., 2003, "Design and Analysis of remote center of compliance structures," Journal of Field Robotics, Vol. 20, Issue 8, pp. 415-427.

[8] Bellouard, Y., 2010, Microrobotics, Methods and applications, CRC press, Boca Raton, Florida, pp. 200-202.

[9] Zhao, B., Nelson, C., 2015, "Sensorless Force Sensing for Minimally Invasive Surgery," ASME J. Med. Devices, Vol. 9, Issue 4, p. 041012-041012-14. doi: 10.1115/1.4031282

[10] Trease, B. P., Moon, Y. M., Kota, S., 2004, "Design of large displacement compliant joints," J. Mech. Des., Vol. 127, Issue 4, pp. 788-798.

[11] Bedem, L. V. D., 2010, "Realization of a Demonstrator Slave for Robotic Minimally Invasive Surgery", Ph.D. Thesis, Eindhoven University of Technology, The Netherlands.

[12] Howell, L., Magleby, S. P., 2013, Handbook of compliant mechanisms, Wiley, New York, NY, pp. 109 -121.

[13] Stratasys, Ltd., 2017, "PLA Data Sheet," Stratasys, Eden Prairie, Minnesota, United States, accessed on October 28, 2017, http://www.stratasys.com/PLA.

[14] Gallego, J. A., Herder, J. L., 2010, "Criteria for the Static Balancing of Compliant Mechanisms," ASME IDETC, DETC2010-28469, Vol. 2, pp. 465-473.

[15] Herder, J. L., 2001, "Energy-Free Systems, Theory, Conception and Design of Statically Balanced Spring Mechanisms," Doctoral thesis, Delft University of Technology, Delft, The Netherlands.

[16] Smith, S. T., 2000, Flexures, Elements of Elastic mechanisms, CRC press, Boca Raton, Florida, pp. 204-205.

[17] Aguirre, M., Steinórsson, Á. T., Horeman, T., and Herder, J. L., 2015, "Technology Demonstrator for Compliant Statically Balanced Surgical Graspers," ASME J. Med. Devices, Vol. 9 Issue 2, p.020926. doi:10.1115/1.4030131.

[18] Bruyas, A., Geiskopf, F., Renaud, P., 2014, "Towards statically balanced compliant joints using multimaterial 3D printing," ASME IDETC, DETC 2014-34532.

[19] Fedder, G. K., 1994, "Simulation of Microelectromechanical Systems," Doctoral Thesis, University of California at Berkeley, CA, USA.